atmosphere

MDPI

Brief Report

What Determines the Parameters of a Propagating Streamer: A Comparison of Outputs of the Streamer Parameter Model and of Hydrodynamic Simulations

Nikolai G. Lehtinen [1,*] and Robert Marskar [2]

[1] Birkeland Centre for Space Science, University of Bergen, 5007 Bergen, Norway
[2] SINTEF Energy Research, 7465 Trondheim, Norway; Robert.Marskar@sintef.no
* Correspondence: nikolai.lehtinen@uib.no

Abstract: Electric streamer discharges (streamers) in the air are a very important stage of lightning, taking place before formation of the leader discharge, and with which an electric discharge starts from conducting objects which enhance the background electric field, such as airplanes. Despite years of research, it is still not well understood what mechanism determines the values of a streamer's parameters, such as its radius and propagation velocity. The novel Streamer Parameter Model (SPM) was made to explain this mechanism, and to provide a way to efficiently calculate streamer parameters. Previously, we demonstrated that SPM results compared well with a limited set of experimental data. In this article, we compare SPM predictions to the published hydrodynamic simulation (HDS) results.

Keywords: atmospheric electricity; electric streamer discharges; streamer theory; streamer parameters; plasma instabilities; partially-ionized plasmas

PACS: 52.80.Mg; 92.60.Pw

Citation: Lehtinen, N.G.; Marskar, R. What Determines the Parameters of a Propagating Streamer: A Comparison of Outputs of the Streamer Parameter Model and of Hydrodynamic Simulations. *Atmosphere* **2021**, *12*, 1664. https://doi.org/10.3390/atmos12121664

Academic Editor: Lawrence D. Carey

Received: 29 October 2021
Accepted: 8 December 2021
Published: 11 December 2021

1. Introduction

Electric streamer discharges, or simply streamers, are ionized columns in gas or liquid which advance by ionizing the material in front of them with the enhanced field at the streamer tip [1,2]. They are an important stage in the formation of sparks, and thus, especially those propagating in air, play a huge role both in technology and natural phenomena such as lightning and red sprites. Quantifying streamer properties at high altitudes is important for understanding how lightning interacts with airplanes (e.g., [3,4]). Besides being affected by diverse background conditions, streamer properties may not simply scale in proportion to air density: in particular, the positive streamer threshold field may have nonlinear dependence on air density [5].

Raether [6], Meek [7], and Loeb and Meek [8] were the first to propose that electrons, when undergoing impact ionization avalanche in high electric field in air, create sufficient space charge density to modify the external field, and thus, to form a streamer. In the process of the avalanche-to-streamer transition, electron diffusion plays a crucial role, as it determines the transverse size of the avalanche, and therefore the space charge density. The same authors also proposed the mechanism of streamer propagation in air, which is based on photoionization. The mechanism works in the following way: (1) UV (ultraviolet) photons are generated in the streamer head by de-excitation of N_2; (2) photons propagate forward and ionize O_2 in front of the streamer, thereby creating free electrons; (3) the created electrons seed impact ionization avalanches which propagate in the backward direction in the high field near the streamer tip. This mechanism works for both positive (cathode-directed) and negative (anode-directed) streamers [2] (pp. 335, 338); however, the difference in electron drift direction makes properties of positive and negative streamers very distinct.

The physics determining the parameters of a propagating streamer discharge in air, such as its radius and speed, is a long-standing problem [9]. Even though the lateral spreading of an avalanche is due to electron diffusion in the avalanche-to-streamer transition, it may be shown that diffusion is not the main mechanism due to which a streamer acquires its finite radius [10,11]. In the present work, we calculate the corrections to streamer parameters due to electron diffusion and demonstrate that they are insignificant.

The usual approach to theoretical studies of streamers is the numerical solution of the system of coupled electrostatic and hydrodynamic equations for electric field and electron number density. Such hydrodynamic simulations (HDS) are very computationally intensive, as they need to have many spatial grid cells in order to resolve the thin ionization front well. This is complicated by the need to resolve other spatial scales, which are very different: the streamer head, which may have a radius two orders of magnitude larger than the ionization front thickness, and the streamer length, which may be at least an order of magnitude larger than the radius. Despite considerable development, HDS still remain challenging, as the computational stability and accuracy are achieved only at small grid cell sizes, and therefore, with a large number of cells. There exist even more complicated numerical models that attempt to include kinetic effects, such as particle-in-cell (PIC) and hybrid codes. A brief review of the HDS modeling efforts is given, e.g., in [12].

Low-computational-intensity alternatives to HDS are one-dimensional streamer models [13–15]. However, these models still face the problem of unambiguous selection of parameters of streamer propagation, such as the radius, which has to be specified as an input to the model.

With the Streamer Parameter Model (SPM), we attempted to uncover the mechanism responsible for the emergence of streamer parameters, and at the same time develop an efficient algorithm for their computation. It shares the feature of being relatively low computationally easy with the one-dimensional models mentioned above; however, unlike them, it provides an unambiguous selection of the streamer radius, which is based on this mechanism. In Section 3, we demonstrate that SPM results compare reasonably well to those of HDS. We applied SPM to positive streamers; however, SPM can also make predictions about negative streamers: in particular, the negative streamer threshold field was calculated to be $E_{-t} \approx 1$ MV/m, which was also observed in experiments [2] (p. 362), and according to the theory of Lehtinen [11], is not due to the electron attachment process.

2. Streamer Parameter Model (SPM)

The details of the Streamer Parameter Model (SPM) are given in [11], and also in an unpublished manuscript [16]. Here, we give a quick overview of the key points of the model.

The streamer under consideration grows with velocity V from a planar electrode, in constant uniform electric field E_e ([11] Figure 2). It has a shape of a cylinder (channel), which is attached to the electrode on one end and has a hemispherical cap (head) of the same radius on the other end. The total length of the streamer is L, and the radius of both the head and the channel is a. The electron number density on the axis and electric field inside the streamer are both assumed to be constant and have values of n_s and E_s, respectively. The validity of these assumptions is discussed in Section 4.1.

SPM describes a streamer of given length L, in given external field E_e, with the following five unknown parameters: the radius, a, the velocity, V, the field inside the channel, E_s, the electron number density on the axis of the channel, n_s, and the maximum field at the tip, E_m. These parameters are coupled to each other by the following relations:

- SPM1: Electrostatic relationship between E_e, E_m, E_s: the field at the streamer tip is enhanced because of available voltage due to difference in E_e and E_s: $\Delta U = (E_e - E_s)L$.
- SPM2: Current continuity at the streamer tip: the conductivity current inside the streamer becomes displacement current outside.
- SPM3: Ionization and relaxation balance: the ionization time scale in the region of the highest electric field at the streamer tip is approximately equal to the Maxwellian charge relaxation time inside the streamer.

- SPM4: Photo-ionization and impact ionization balance, which provides the relation between V and a.

The algebraic equations corresponding to these relations and the references to the works in which they were originally discussed are given in Lehtinen [11].

The system of equations SPM1–SPM4 is sufficient to uniquely determine the set of streamer parameters only if the radius, a, is fixed. This led Lehtinen [11] to introduce the notion of "streamer modes" by analogy with the normal oscillation modes in a linear system. A familiar example of such a system is an unstable uniform plasma with infinitesimal perturbations, such as a plasma penetrated by a uniform electron beam. Such a system also possesses a free parameter, namely, the wavelength of a perturbation (if we constrain ourselves to axially-symmetric perturbations only). Incidentally, this parameter, like a, also has the dimensionality of length. For any given wavelength, the instability growth rate, and the proportionality coefficients among amplitudes of perturbations of electric field, electron number density, etc., may be determined. When an unstable linear system develops in time, starting from a random fluctuation with a broad spectrum of wavelengths, only one mode at a single wavelength (the "preferred" mode), which has the highest growth rate, i.e., is the most unstable, survives in the long run. A less familiar example of an unstable linear system, though more relevant to the streamer studies, is the planar ionization front and its infinitesimal transverse perturbations. Derks et al. [17] have calculated the unstable modes and found the preferred mode in this system. Their model included electron drift and diffusion, but not photoionization. Unlike these examples, system SPM1–SPM4 is highly nonlinear, and the closest analogy to the growth rate that we can find is the streamer velocity, V. Thus, we propose that the parameters of a physical streamer are described by the system of equations SPM1–SPM4, with a "preferred" or "most unstable" radius a at which V is maximized. Selection of the preferred radius by the maximization of velocity may be used in one-dimensional streamer models [13–15] (see also suggestions in Section 4.1 for the future developments of SPM).

Function $V(a)$ is an analog of a "dispersion function", which couples the temporal and the spatial scale of the system. It is worth noting that the dependence $V(a)$ indeed has a shape with a maximum, and all other parameters (E_s, n_s, E_m) have monotonic dependence on a [16]. This peculiar shape of $V(a)$ may be given the following simplified explanation. Velocity is related to the streamer radius by relation SPM4. There exists an approximate version of this relation, first noticed by Loeb [18], which we will now derive. The ionization front thickness (i.e., the avalanche length in the streamer reference frame), d, is related to the radius, a, by $a/d = N_a$, where $N_a \approx 8$ [10] is the number of avalanche lengths required to boost the small number density of photoelectrons ahead of the streamer up to the high electron number density in the channel, n_s. On the other hand, $d \approx V/\nu_t(E_m)$, where $\nu_t(E_m)$ is the net ionization rate, taken at the maximum field (see more discussion in Section 4.2). Thus, the velocity, V, is related to the radius approximately as $V \approx a\nu_t(E_m)/N_a$ [18]. At small radii, even though E_m, and therefore, $\nu_t(E_m)$, is high, proportionality $V \propto a$ dominates, and V declines with decreasing a. On the other hand, at large radii a, the field enhancement at the streamer tip (determined by SPM1) becomes smaller. The smaller field yields a smaller ionization rate $\nu_t(E_m)$, thus V again declines. We do not exclude the possibility that there exists a gas in which ν_t does not decline fast enough with growing a, resulting in $V(a)$ not having a maximum. SPM predicts that, in such a gas, formation of a streamer discharge would be impossible.

In our earlier work [11], we compared SPM predictions to limited experimental results by Allen and Mikropoulos [19]. Only velocity at streamer length $L = 12$ cm was compared in a wide range of background fields E_e, with the differences not exceeding $\sim$30%. In this work, we compare SPM to hydrodynamic simulations (HDS), which were performed by several research groups and presented by Bagheri et al. [12]. The mentioned study was chosen because (1) having several research groups perform the same study makes the results more reliable, reducing the chance of accidental HDS inaccuracies; and (2) the conditions chosen for streamer propagation (constant, uniform external field, low electron attachment)

are relatively easily translated into SPM. The comparison of SPM with HDS is grounded in the hypothesis that in HDS, as in nature, the preferred, i.e., the most unstable, mode of the streamer propagation is also selected. We have also enhanced the SPM model compared to our previous work [11] by allowing it to include electron diffusion and background electron density. The theory behind these enhancements is presented in the Appendix A.

SPM calculations were run on a desktop computer with an 8-core Intel(R) i7-4790 3.60 GHz CPU. All the streamer parameters were calculated independently for each set of values for external field and streamer length (E_e, L), because SPM suggests that the streamer parameters are independent from the previous history of the streamer propagation. Each calculation takes about 10–20 s on a single processor, and may be performed using the instructions at the link given in the Data Availability Statement.

3. Results

We considered the same three test cases as Bagheri et al. [12] for positive streamers in dry air at 1 bar and 300 K:

1. No photoionization; presence of relatively high background free electron number density of $n_e = 10^{13}$ m^{-3}.
2. No photoionization; presence of relatively low $n_e = 10^9$ m^{-3}.
3. With photoionization and $n_e = 10^9$ m^{-3}. Photoionization is treated with three different approximations to the original description by Zheleznyak et al. [20]. These approximations are described in detail in (Bagheri et al. [12] Appendix A). In this article, we label them as "Luque", "Bourdon2", and "Bourdon3", similarly to [12].

The goal of the first two cases, according to Bagheri et al. [12], was to compare robustness of HDS algorithms. The second case, with a much smaller n_e, creates much steeper gradients in the ionization front than the first one, making it computationally much more challenging.

Streamer discharges in HDS [12] were simulated between planar electrodes in a square domain with a radius and height of 1.25 cm, with background electric field of $E_e = 1.5$ MV/m. In SPM, however, we only took into account the planar anode, and thus did not reproduce the effects of the image charges induced in the cathode or any effects due to the side walls of the simulation domain. In HDS, the positive streamer was started by a small Gaussian-shaped ionized region (with radius of 0.4 mm and maximum electron number density of 5×10^{18} m^{-3}), centered at the small distance of 0.25 cm from the anode. The radius of the initial ionization region was larger than the streamer radii during most stages of streamer development, as calculated by both SPM and HDS (see Figures 1–3, panels d). This suggests that the initial radius does not play a large role in the subsequent development, supporting the SPM hypothesis that streamer parameters are mostly determined by the external field, E_e, and the streamer length, L.

Since the background ionization cannot be neglected, it being the only source of free electrons in Cases 1 and 2, in the Appendix A we have derived Equation (A2), which replaces the photoionization-impact ionization balance equation SPM4. It may include the electron diffusion as a small correction, which is also derived in the Appendix A.

For consistency, we used the same functional dependence on electric field E of ionization rate ν_i, attachment rate ν_a, electron mobility μ and electron diffusion coefficient D as Bagheri et al. [12]. (In this article, we often use quantities which are derived from these, namely, the net ionization rate, $\nu_t = \nu_i - \nu_a$, and the electron drift velocity, $v = \mu E$.) To model photoionization in Case 3, we used the same approximations as Bagheri et al. [12] instead of the original Zheleznyak et al. [20] expression, which was used in [11].

3.1. Case 1

The first test case included a relatively high background number density of electrons and ions $n_e = 10^{13}$ m^{-3} without photoionization. The results are presented in Figure 1. The black lines reproduce the HDS results presented by Bagheri et al. [12]. The maximum field E_m presented in Figure 1b, and the radius, a, presented in Figure 1d, are two of the parameters for which the system SPM1–SPM4 was solved, i.e., the immediate outputs of

the SPM. The other plots are derived as follows. The streamer length L as a function of time t in Figure 1a was calculated by solving $dL/dt = V(L)$, where $V(L)$ is the output of SPM. The total number of electrons N in Figure 1c was calculated from SPM results as

$$N = \frac{1}{2}\pi a^2 L n_s.$$

The factor of $1/2$ came from the assumption that the electron number density falls off parabolically towards the walls of the streamer channel, i.e., $n(r) = n_s[1 - (r/a)^2]$.

Unfortunately, the HDS results for the streamer radius, a, as a function of L, were not available for Case 1 for all participating HDS teams in the form of a plot in [12] (however, they were available for Cases 2 and 3). We extracted the approximate values of L and a from time snapshots in Figure 3 of [12], produced by one of the participating teams.

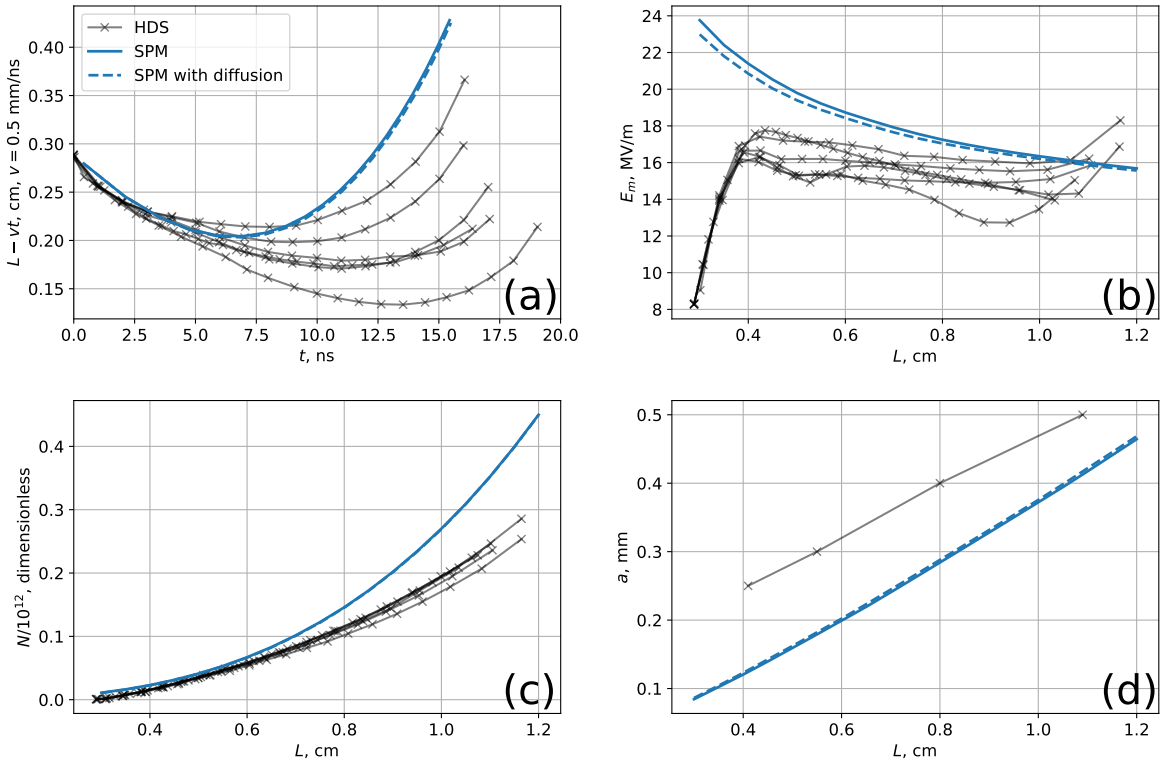

Figure 1. Case 1: Initial background electron number density $n_e = 10^{13}$ m^{-3}, and no photoionization: (**a**) length L as a function of time t; (**b**) maximum electric field E_m as a function of length; (**c**) total number of produced electrons N as a function of length; (**d**) streamer radius a as a function of length (HDS results for one team only). Dashed lines denote SPM results with diffusion. HDS results in panels (**a**–**d**) were adapted from Figures 5b, 6a,b and 3 in Bagheri et al. [12].

For sufficiently fine grids, good agreement was reached between several HDS codes [12]. We observed that SPM also produces reasonable agreement with HDS, reproducing the same qualitative features:

1. Velocity V in Figure 1a grows with streamer length (and with time).
2. Maximum electric field E_m decreases with streamer length L, at least for the middle values of L (the discrepancies at low and high L are discussed below).
3. Number of electrons N grows with L; the rate of growth also increases with L.
4. Radius a grows with length L.

Notably, in Figure 1d, the radius a in SPM was generally smaller than that in HDS. This may be due to the approximation made in SPM that the radius is constant along the channel and is also equal to the curvature radius of the streamer head at the tip. In Section 4.1, we

discuss this approximation and suggest that a in SPM more closely corresponds to the tip curvature radius, which may be smaller than the channel radius.

In addition to discrepancies caused by approximations in the SPM (see Section 4.1), additional discrepancies between the SPM and HDS are caused by the HDS simulation conditions which were different from the "ideal" conditions used in SPM:

1. The HDS did not start at zero L, namely, it started with a small ionized region in the vicinity of the anode. This caused the field E_m to gradually rise until the streamer was formed (see the low L values in Figure 1b). SPM, on the other hand, provided results only with the streamer already formed.
2. At large L, the discrepancy is due to the proximity of the opposite electrode (cathode). The negative image charge of the streamer head, induced in the conducting cathode, enhanced the field in HDS (Figure 1b). The cathode, as we already mentioned, was not taken into account in the SPM.

The effect of electron diffusion is included in SPM according to the prescription derived in the Appendix A. SPM results with diffusion are shown with dashed lines in Figure 1. We observed that the effect of diffusion is quite small, confirming our estimates in the Appendix A and the suggestion of Naidis [10] that it does not affect the streamer propagation.

3.2. Case 2

In the second case, the background electron number density was $n_e = 10^9$ m^{-3}. The results are presented in Figure 2, with the same notation as in Figure 1. The lower value of n_e created much steeper gradients in the ionization front, which made HDS computations quite challenging [12]: oscillations in the streamer properties, branching, and numerical instabilities were observed. By using a finer grid spacing, some groups were able to reach reasonable agreement in their results, without oscillations. Again, SPM produces reasonable agreement with HDS.

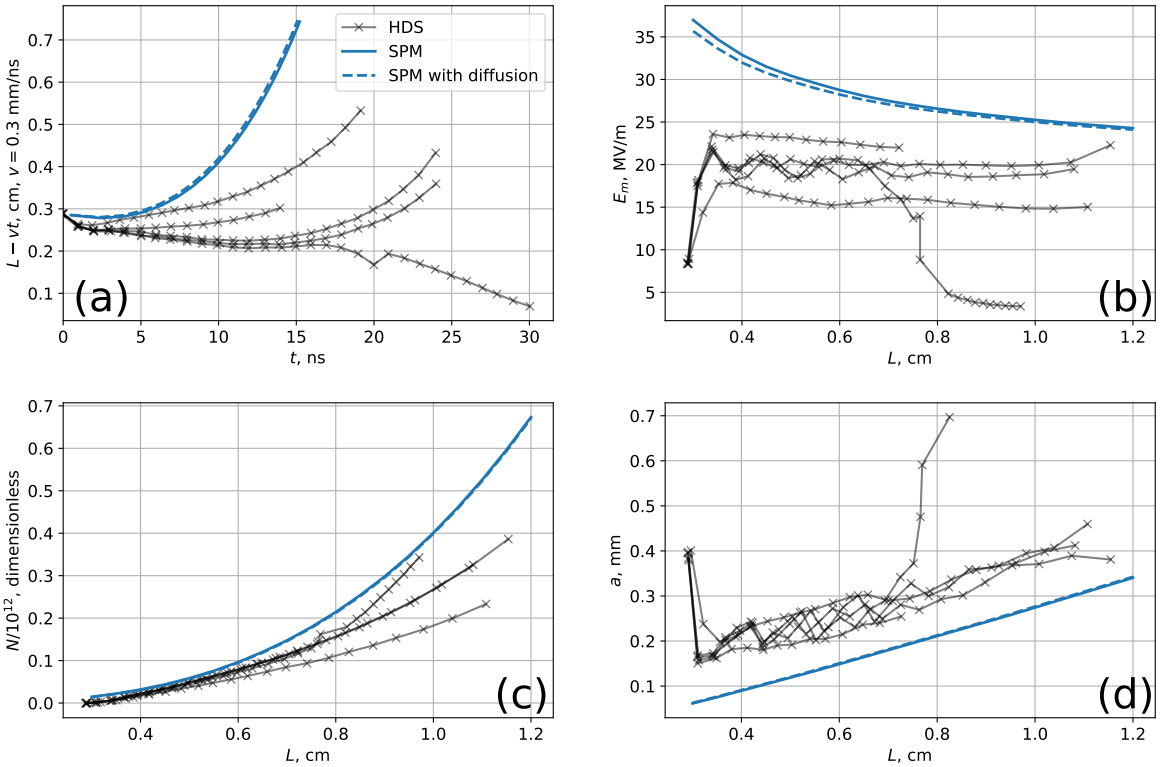

Figure 2. Case 2: Initial background electron number density $n_e = 10^9$ m^{-3}, and no photoionization: (**a**) length L as a function of time t; (**b**) maximum electric field E_m as a function of length; (**c**) total number of produced electrons N as a function of length; (**d**) streamer radius a as a function of length. Dashed lines denote SPM results with diffusion. HDS results in panels (**a**–**d**) were adapted from Figures 8, 9a,b and 10 in Bagheri et al. [12].

However, SPM mostly produced higher fields E_m than HDS, as seen in Figure 2b. This could be due both to errors from approximations made in SPM (see Section 4.1) and simulation conditions differences, listed in Section "Case 1". The challenges in HDS, caused, e.g., by the fact that higher E_m requires smaller grid step Δx, are discussed in Section 4.2. From that discussion, it seems that convergence to the correct solution at $\Delta x \to 0$ was achieved, at least by some of the HDS. The higher field in SPM also led to higher velocity V and smaller radius a than in HDS. However, the smaller radius in SPM may be also due to the difference in definitions of the radius: SPM uses the radius of curvature, and not the channel radius, which may be wider, similarly to Case 1 (see also Section 4.1).

3.3. Case 3

The third test case includes both small background electron number density $n_e = 10^9$ m^{-3} and photoionization. The photoionization in SPM is implemented in three different approximations, described in (Bagheri et al. [12] Appendix A) and labeled in Figure 3 as "Luque", "Bourdon2", and "Bourdon3". The numerical differences in HDS between different teams were more significant than differences due to the type of approximation [12]. Thus, only "Bourdon3" approximation HDS results are shown in Figure. The differences in $L(t)$ and $E_m(L)$ due to photoionization approximation choice were presented in Figure 16 of [12]. However, they were too small to draw parallels with analogous differences in SPM.

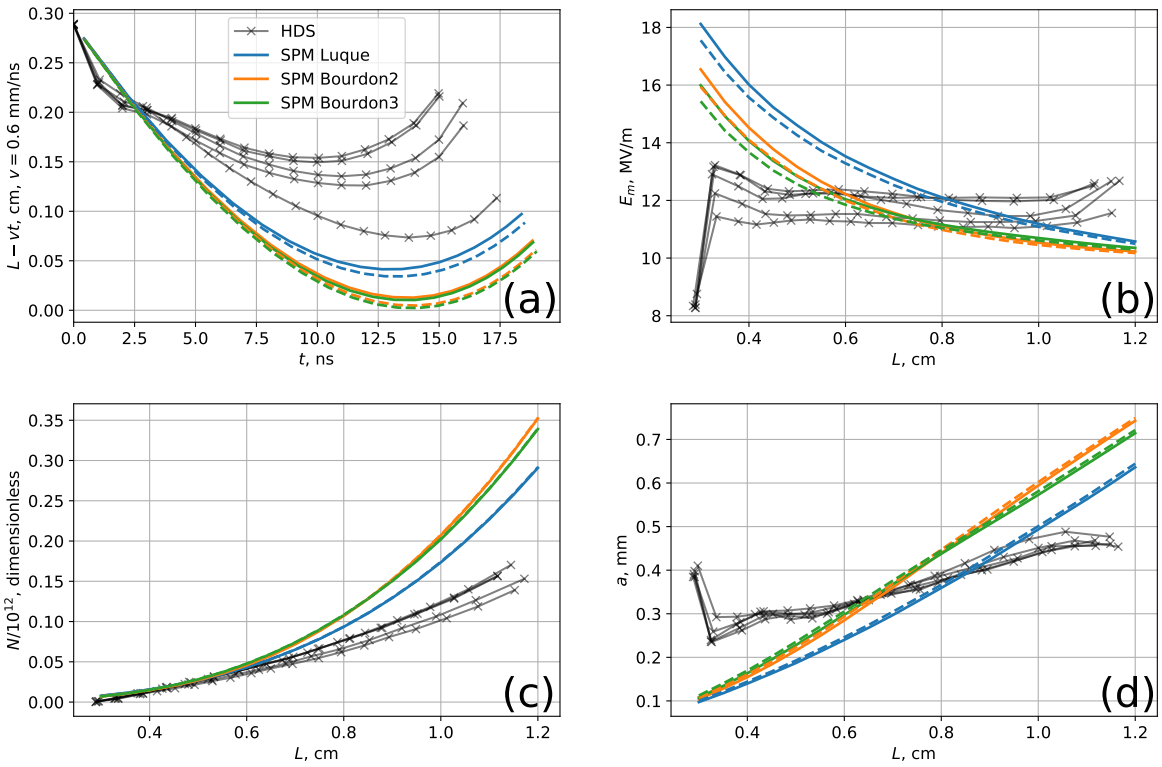

Figure 3. Case 3: Photoionization is present, initial background electron number density is $n_e = 10^9$ m^{-3}: (**a**) length L as a function of time t; (**b**) maximum electric field E_m as a function of length; (**c**) total number of produced electrons N as a function of length; (**d**) streamer radius a as a function of length. Dashed lines denote SPM results with diffusion. HDS results in panels (**a**–**d**) are adapted from Figures 13, 14a,b and 15 in Bagheri et al. [12].

4. Discussion

4.1. Possible Errors Due to Approximations in SPM

Even though SPM, due to the absence of any discretization used in HDS, does not have a problem with a steep gradient, there can be significant errors due to approximations made when we reduce a complicated hydrodynamic/electrostatic problem to a small system of

algebraic equations SPM1–SPM4. They were discussed in detail by Lehtinen [11], so we just briefly mention them here:

1. The radius, a, enters the system of SPM1–SPM4 in relations that describe processes at the tip of the streamer. Therefore, the value of a is more relevant to the tip curvature radius, than to the possibly different radius of the channel.
2. We assumed that $n_s = const$ along the axis of the channel. At low external fields E_e, especially those close to the positive streamer threshold $E_{+t} \approx 0.45$ MV/m [2] (p. 362), the number of electrons in the channel declines due to attachment. However, for the field $E_e = 1.5$ MV/m, used in this work, attachment in the channel can be neglected, especially when using the attachment coefficient expression from Bagheri et al. [12] which gives lower values than we would get if the 3-body attachment process were included.
3. Assumption of $E_s = const$ along the channel follows from $n_s = const$ taken together with the assumption of constant current, $J = en_s v(E_s) = const$.

The last assumption deserves more discussion as it may not be valid in some situations. By taking the channel current to be constant along the channel, we assumed that the surface charges on the walls of the channel do not change as the streamer grows, and the new charges are formed only at its head. This assumption seems to be valid for propagating streamers, but breaks down, e.g., for steady-state streamer propagation at E_{+t} [21,22], in which the charges on the walls of the channel change with time, namely, drop to zero towards the tail of a finite-length streamer as it moves through the air. In the future versions of SPM, we plan to include E_s and n_s not as single numbers, but as one-dimensional variables that vary along the channel, in order to correctly describe such situations. This will allow one to study, e.g., the nature of positive streamer threshold field and positive streamer inception. Understanding and predicting electric field thresholds for streamer inception in diverse conditions inside clouds is going to contribute to understanding airplane-lightning interactions. However, in [12], the attachment role was insignificant, which allowed us to neglect the variation of n_s (and, therefore, E_s) along the channel and to use the present simpler version of SPM.

4.2. Shortest Spatial Scale in a Streamer and in HDS

The shortest spatial scale in a streamer is found at the streamer front, which has the highest gradient of electron number density and electric field. This scale is given by the thickness of the ionization front, d, and is related (but not equal) to the shortest impact ionization avalanche length, $d_0 = 1/\alpha_t(E_m)$, where α_t is the net ionization coefficient (also called net Townsend coefficient), taken at the maximum field, E_m. We may estimate d as [11]

$$d = \frac{V \pm v(E_m)}{\nu_t(E_m)} = \left[\frac{V}{v(E_m)} \pm 1\right] d_0,$$

where $\nu_t = v\alpha_t$ is the net ionization rate, $v(E)$ is the electron drift velocity, and the upper (lower) sign is for a positive (negative) streamer. The elongation ($d > d_0$) in the case of the positive streamer is due to the fact that the backward electron velocity in respect to the moving ionization front is $V + v(E_m)$. Usually the streamer speed is rather high, so that $V \gg v(E_m)$ and $d \gg d_0$. However, under some conditions (examples given below) the streamer speed is low, so it is possible to have $d \approx d_0$. For negative streamers, it is even possible to have $d < d_0$ when V happens to be in the interval $v(E_m) < V < 2v(E_m)$. Incidentally, it is impossible to have $V < v(E_m)$ because then d would be negative, making it impossible for electron number density to grow from low values ahead of the streamer to a high value in the streamer head. This may be the underlying reason for the negative streamer threshold of $E_{-t} \approx 1$ MV/m, which was calculated by Lehtinen [11].

The ionization front thickness is the shortest spatial scale that needs to be resolved in discretized solution methods, such as HDS. The usual criterion for the choice of the grid step, Δx, used in HDS is [12,23–26]:

$$\alpha_t(E)\Delta x = C, \qquad C \lesssim 1. \tag{1}$$

(An alternative criterion is to choose Δx on the basis of how quickly the gradients of calculated values change, used, e.g., by Lehtinen and Østgaard [27]). At the streamer front, this is equivalent to $d_0/\Delta x = 1/C$, or

$$\frac{d}{\Delta x} = \frac{V/v(E_m) \pm 1}{C} = N_g,$$

i.e., the ionization front thickness is resolved by N_g spatial grid points. For a usual situation, $V \gg v(E_m)$, criterion (1) works well even for $C \sim 1$, because even then $N_g \gg 1$. However, for short or narrow streamers, which propagate slowly, velocity V is rather low and may be even lower than the electron drift speed, $v(E_m)$. Below the positive streamer threshold, E_{+t}, the propagating streamers slow down and eventually stop [22]. When such streamers stop propagating, in addition to declining velocity V, we also have a shrinking radius, $a \to 0$, and increasing electric field, $E_m \to \infty$, which exacerbates the situation, because d_0 decreases as well. In such situations, the non-local effects [28] also need to be incorporated into the HDS model.

In Case 2 at length $L = 0.35$ cm, the SPM-predicted electric field $E_m \approx 35$ MV/m (see Figure 2b), the velocities were $V \approx 0.3$ mm/ns, and $v(E_m) \approx 0.9$ mm/ns, so $d \sim d_0$ and the ionization front was not well resolved when criterion (1) was used with $C \approx 1$ because then $N_g \approx 1$. The situation was improved for a longer (and wider) streamer: when $L = 1$ cm in Case 2, the SPM field $E_m \approx 25$ MV/m, $V \approx 1$ mm/ns, and $v(E_m) \approx 0.72$ mm/ns, so $N_g \approx 2.4$ for $C = 1$. The resolution of the ionization front, therefore, was better for a longer streamer with $L = 1$ cm than for a shorter one with $L = 0.35$ cm. Unfortunately, to get to a longer (and wider) streamer, in this particular case, the simulation had first to go through the stage with a shorter (and narrower) streamer.

Even though these considerations suggest that the choice of the grid step presented challenges in HDS simulations of Case 2, we do not know the accuracy of the solutions, and thus do not have enough information to state that these challenges were one of the sources of discrepancy. The numerical errors depend also on the choice of the discretization scheme of Poisson and advection-diffusion equations: higher-order methods in both time and space reduce numerical errors, even when N_g is small. Results presented in Figure 11 of Bagheri et al. [12] may suggest that the numerical errors in HDS were not large enough to cause the discrepancies between HDS and SPM results for Case 2. In that Figure, it is shown that the values of E_m at resolution $\Delta x = 0.8$ μm were only about 5% higher than those at $\Delta x = 1.5$ μm. For comparison, at the maximum $E_m \approx 23$ MV/m obtained in HDS, $d_0 \approx 2.7$ μm.

5. Conclusions

In SPM, the physical streamer emerged by selection out of all the possible streamer modes, satisfying the simplified system SPM1–SPM4, as the one with the highest possible velocity. The streamer parameters are determined uniquely in SPM, and are dependent only on the external field E_e and the streamer length L, and thus are independent of the preceding history of streamer development. We have demonstrated that SPM produces results which are generally in good agreement with HDS. The comparisons with HDS in Figures 1–3 demonstrate that sometimes the discrepancies between different HDS codes were in the same order as the discrepancies between SPM and HDS. Most discrepancies between SPM and HDS, notably in Figure 2, were probably caused by the crudeness of the simplifying assumptions in SPM. Some of the discrepancies, however, were due to the different conditions of the problem (streamer starting not from zero length; presence of the

opposite electrode). The largest discrepancies were for the case in Figure 2, which, according to Bagheri et al. [12], was also challenging for HDS. Inclusion of electron diffusion changed the results insignificantly. We conclude that SPM, despite the crudeness of the model, provides a computationally simple way to reliably assess streamer properties. The future versions of SPM will provide more flexibility in choosing background conditions and more accurate description of processes in the streamer channel.

Author Contributions: Streamer Parameter Model, writing, discussion, N.G.L.; writing, discussion, R.M. All authors have read and agreed to the published version of the manuscript.

Funding: This study was supported by the European Research Council under the European Union's Seventh Framework Programme (FP7/2007-2013)/ERC, grant agreement number 320839 and the Research Council of Norway under contracts 208028/F50, 216872/F50, and 223252/F50 (CoE). R.M. acknowledges funding from the Research Council of Norway, grant number 319930/E20.

Institutional Review Board Statement: Not applicable.

Informed Consent Statement: Not applicable.

Data Availability Statement: The Python3 scripts necessary for running SPM and needed to reproduce the results of this paper are available at https://gitlab.com/nleht/streamer_parameters, accessed on 10 December 2021.

Conflicts of Interest: The authors declare no conflict of interest.

Abbreviations

The following abbreviations are used in this manuscript:

SPM	Streamer Parameter Model
HDS	Hydrodynamic simulation(s)
UV	Ultraviolet

Appendix A

We solve the following continuity equation for electron number density n, in the presence of impact ionization, diffusion and photoionization:

$$-\partial_\xi([V \pm v]n) = \nu_t n + \partial_\xi\left[D\partial_\xi n\right] + s_{\mathrm{ph}}(\xi). \tag{A1}$$

We use the same notation as Lehtinen [11]: V is the streamer velocity; $\xi = x - Vt$ is the co-moving coordinate along the streamer axis, with $\xi = 0$ corresponding to the streamer front; ∂_ξ denotes the derivative in respect to ξ; $n(\xi)$ is the electron number density on the axis; v is the electron drift velocity; ν_t is the net ionization rate; $s_{\mathrm{ph}}(\xi)$ is the source of free electrons due to photoionization. The upper (lower) sign is for a positive (negative) streamer. In addition to terms included by Lehtinen [11], we introduced the diffusion term with coefficient D. Values of ν_t, v, D are functions of electric field E, which, in turn, is a function of ξ.

If the diffusion term is neglected, the solution of (A1) is

$$n(\xi) = \frac{1}{V \pm v}\int_\xi^\infty s_{\mathrm{ph}}(\xi')\exp\left\{\int_\xi^{\xi'}\frac{\nu_t\,d\xi''}{V \pm v}\right\}d\xi' + \frac{C}{V \pm v}\exp\left\{\int_\xi^\infty \frac{\nu_t\,d\xi'}{V \pm v}\right\}.$$

The integration constant, $C = n_e[V \pm v(E_e)]$, is obtained from the boundary condition $n(\infty) = n_e$, where n_e is the initial background electron number density. By equating $n(0) = n_s$, we get the following condition:

$$\int_0^\infty K_{a_{\mathrm{ph}}}(\xi)e^{\gamma(\xi)}\,d\xi + \frac{n_e[V \pm v(E_e)]}{n_s[V \pm v(E_s)]}e^{\gamma(\infty)} = 1, \quad \text{where } \gamma(\xi) = \int_0^\xi \frac{\nu_t\,d\xi'}{V \pm v}. \tag{A2}$$

Without photoionization (the first term on the left-hand side) this expression is the same as Equation (4) of Naidis [10]; without background electrons (the second term) it is the same as SPM4 equation of (Lehtinen [11] Section 4.6, item 4), compare to the similar expression of (Pancheshnyi et al. [29] Equation (17)). Thus, (A2) should be used instead of SPM4 in the system SPM1–SPM4, when background electron number density $n_e \neq 0$.

Function $K_{a_{\rm ph}}(\xi)$ is given by

$$K_{a_{\rm ph}}(\xi) = \frac{s_{\rm ph}}{n_s[V \pm v(E_s)]} = \int_{r_\perp < a_{\rm ph}} K(r)\, d^2\mathbf{r}_\perp, \qquad \text{where } r = \sqrt{\xi^2 + r_\perp^2},$$

and is dependent only on ξ and $a_{\rm ph}$, which is the effective streamer head radius when it acts as the source of photons (Lehtinen [11] assumed $a_{\rm ph} = a/2$), and $K(r)$ is the kernel of the integral transform which turns $S_i = \nu_i n \approx \nu_t n$ into $s_{\rm ph}$ [20]. In HDS, $K(r)$ is a Helmholtz approximation to the Zheleznyak et al. [20] model ([12] Appendix A).

Let us now tackle the correction due to diffusion and demonstrate that it is small. From now on, we neglect the photoionization term in (A1), since the diffusion is important only in the region where n is already high and the impact ionization term dominates as the source of free electrons. Substitute

$$\partial_\xi n = -\frac{\nu_t \pm \partial_\xi v}{V \pm v} n$$

into the diffusion term in (A1) and transfer it to the left-hand side:

$$-\partial_\xi \left(\left[V \pm v - D \frac{\nu_t \pm \partial_\xi v}{V \pm v} \right] n \right) = \nu_t n.$$

This looks like (A1) without diffusion, with substitution

$$V \pm v \longrightarrow (V \pm v)\left(1 - \frac{D(\nu_t \pm \partial_\xi v)}{(V \pm v)^2}\right),$$

which we can also make in formula (A2) to get condition SPM4 in the next order of approximation. For $V \gtrsim 0.3$ Mm/s, $\nu_t \lesssim 10^{11}$ s^{-1} (which is valid for $E \lesssim 15$ MV/m), $D \approx 0.1$ m^2/s and with estimated values of $|\partial_\xi v| \lesssim v/a$ for $a \gtrsim 0.1$ mm, the correction multiplication factor is different from unity by no more than 10%, which justifies this perturbation approach.

References

1. Bazelyan, E.M.; Raizer, Y.P. *Spark Discharge*; CRC Press: New York, NY, USA, 1998.
2. Raizer, Y.P. *Gas Discharge Physics*; Springer: Berlin, Germany, 1991.
3. van Deursen, A.; Kochkin, P.; de Boer, A.; Bardet, M.; Allasia, C.; Boissin, J.F.; Flourens, F. Lightning current distribution and hard radiation in aircraft, measured in-flight. In Proceedings of the 2017 International Symposium on Electromagnetic Compatibility—EMC EUROPE, Angers, France, 4–8 September 2017; pp. 1–4. [CrossRef]
4. Skeie, C.A.; Østgaard, N.; Lehtinen, N.G.; Sarria, D.; Kochkin, P.; de Boer, A.I.; Bardet, M.; Allasia, C.; Flourens, F. Constraints on Recoil Leader Properties Estimated from X-ray Emissions in Aircraft-Triggered Discharges. *J. Geophys. Res. Atmos.* **2020**, *125*, e2019JD032151. [CrossRef]
5. Phelps, C.T.; Griffiths, R.F. Dependence of positive corona streamer propagation on air pressure and water vapor content. *J. Appl. Phys.* **1976**, *47*, 2929–2934. [CrossRef]
6. Raether, H. Die Entwicklung der Elektronenlawine in den Funkenkanal. *Z. Phys.* **1939**, *112*, 464–489. [CrossRef]
7. Meek, J.M. A Theory of Spark Discharge. *Phys. Rev.* **1940**, *57*, 722–728. [CrossRef]
8. Loeb, L.B.; Meek, J.M. *The Mechanism of the Electric Spark*; Stanford University Press: Stanford, CA, USA, 1941.
9. Ebert, U.; Sentman, D.D. Streamers, sprites, leaders, lightning: From micro- to macroscales. *J. Phys. D Appl. Phys.* **2008**, *41*, 230301. [CrossRef]
10. Naidis, G.V. Positive and negative streamers in air: Velocity-diameter relation. *Phys. Rev. E* **2009**, *79*, 057401. [CrossRef]
11. Lehtinen, N.G. Physics and mathematics of electric streamers. *Radiophys. Quantum Electron.* **2021**, *64*, 11–25. [CrossRef]
12. Bagheri, B.; Teunissen, J.; Ebert, U.; Becker, M.M.; Chen, S.; Ducasse, O.; Eichwald, O.; Loffhagen, D.; Luque, A.; Mihailova, D.; et al. Comparison of six simulation codes for positive streamers in air. *Plasma Sources Sci. Technol.* **2018**, *27*, 095002. [CrossRef]

13. Aleksandrov, N.L.; Bazelyan, E.M. Temperature and density effects on the properties of a long positive streamer in air. *J. Phys. D Appl. Phys.* **1996**, *29*, 2873–2880. [CrossRef]
14. Guo, J.M.; Wu, C.H. Streamer radius model and its assessment using two-dimensional models. *IEEE Trans. Plasma Sci.* **1996**, *24*, 1348–1358. [CrossRef]
15. Pavan, C.; Martinez-Sanchez, M.; Guerra-Garcia, C. Investigations of positive streamers as quasi-steady structures using reduced order models. *Plasma Sources Sci. Technol.* **2020**, *29*, 095004. [CrossRef]
16. Lehtinen, N.G. Electric streamers as a nonlinear instability: The model details. *arXiv* **2020**, arXiv:2003.09450.
17. Derks, G.; Ebert, U.; Meulenbroek, B. Laplacian Instability of Planar Streamer Ionization Fronts—An Example of Pulled Front Analysis. *J. Nonlinear Sci.* **2008**, *18*, 551–590. [CrossRef]
18. Loeb, L.B. Ionizing Waves of Potential Gradient. *Science* **1965**, *148*, 1417–1426. [CrossRef] [PubMed]
19. Allen, N.L.; Mikropoulos, P.N. Dynamics of streamer propagation in air. *J. Phys. D Appl. Phys.* **1999**, *32*, 913–919. [CrossRef]
20. Zheleznyak, M.B.; Mnatsakanyan, A.K.; Sizykh, S.V. Photo-ionization of nitrogen and oxygen mixtures by radiation from a gas-discharge. *High Temp. (USSR)* **1982**, *20*, 357–362.
21. Francisco, H.; Bagheri, B.; Ebert, U. Electrically isolated streamer heads formed by strong electron attachment. *Plasma Sources Sci. Technol.* **2021**, *30*, 025006. [CrossRef]
22. Pancheshnyi, S.V.; Starikovskii, A.Y. Stagnation dynamics of a cathode-directed streamer discharge in air. *Plasma Sources Sci. Technol.* **2004**, *13*, B1–B5. [CrossRef]
23. Villa, A.; Barbieri, L.; Gondola, M.; Leon-Garzon, A.R.; Malgesini, R. Mesh dependent stability of discretization of the streamer equations for very high electric fields. *Comput. Fluids* **2014**, *105*, 1–7. [CrossRef]
24. Teunissen, J.; Ebert, U. Simulating streamer discharges in 3D with the parallel adaptive Afivo framework. *J. Phys. D Appl. Phys.* **2017**, *50*, 474001. [CrossRef]
25. Marskar, R. An adaptive Cartesian embedded boundary approach for fluid simulations of two- and three-dimensional low temperature plasma filaments in complex geometries. *J. Comput. Phys.* **2019**, *388*, 624–654. [CrossRef]
26. Marskar, R. 3D fluid modeling of positive streamer discharges in air with stochastic photoionization. *Plasma Sources Sci. Technol.* **2020**, *29*, 055007. [CrossRef]
27. Lehtinen, N.G.; Østgaard, N. X-ray emissions in a multi-scale fluid model of a streamer discharge. *J. Geophys. Res. Atmos.* **2018**, *123*, 6935–6953. [CrossRef]
28. Naidis, G.V. Effects of nonlocality on the dynamics of streamers in positive corona discharges. *Tech. Phys. Lett.* **1997**, *23*, 493–494. [CrossRef]
29. Pancheshnyi, S.V.; Starikovskaia, S.M.; Starikovskii, A.Y. Role of photoionization processes in propagation of cathode-directed streamer. *J. Phys. D Appl. Phys.* **2001**, *34*, 105–115. [CrossRef]